



Research Paper / Makale

Thermodynamic and performance evaluation of an integrated geothermal energy based multigeneration plant

Yunus Emre YUKSEL

Afyon Kocatepe University, Education Faculty, Math and Science Education, ANS Campus, Afyonkarahisar, 03200, Turkey, yeyuksel@aku.edu.tr

Received/Geliş: 19.11.2019

Accepted/Kabul: 17.02.2020

Abstract: In this study, a new integrated geothermal energy-based plant is proposed for multigeneration purposes such as hydrogen, electricity, hot water, drying, cooling and heating. Therefore, this proposed integrated system is consisted of proton exchange membrane electrolyzer, hydrogen compression unit, organic Rankine cycles, single effect absorption cooling cycle, hot water storage tank and a drying unit. Thermodynamic analyses including of energy and exergy analyses have been performed for general evaluation of the proposed system. Energy and exergy efficiencies of whole plant are found as 37.65% and 39.26%, respectively. Exergy destruction rate is one of the important indicators to improve system performance. The largest three exergy destruction rates occur in organic Rankine cycle 1 with 3076 kW, single effect absorption cooling with 2816 kW and hydrogen production and compression with 2658 kW. In addition to these analyses, parametric analyses have been carried out to see how some variables affect system performance and useful product generation. For this reason, the impacts of dead state temperature, geothermal mass flow rate, geothermal source temperature and pinch point temperature of heat exchanger 1 are investigated. Any increase in dead state temperature, geothermal mass flow rate and geothermal source temperature has positive impact on system performance and useful product generation. Increase in pinch point temperature of heat exchanger 1 decreases the system performance. Hydrogen production rate reaches maximum point (0.0024 kg/s) when geothermal mass flow rate is 8.125 kg/s or when geothermal working fluid temperature is 168 °C for this paper.

Keywords : renewable energy, geothermal, thermodynamic, exergy, multigeneration

Jeotermal Enerji Kaynaklı Multi-Jenerasyon Enerji Sisteminin Termodinamik ve Performans Değerlendirmesi

Özet: Bu çalışmada, hidrojen, elektrik, sıcak su, kurutma, ısıtma ve soğutma üretimini amaçlayan jeotermal enerji temelli yeni bir entegre multi-jenerasyon enerji üretim sistemi tasarlanmış ve incelenmiştir. Bu entegre multi-jenerasyon enerji sisteminde proton değişimli membran elektrolizör, hidrojen kompresyon ünitesi, organik Rankine çevrimi, tek etkili absorpsiyonlu soğutma çevrimi, sıcak su depolama tankı ve kurulama ünitesi bulunmaktadır. Önerilen sistemi termodinamik açıdan değerlendirmek için enerji ve ekserji analizleri uygulanmıştır. Sistemin toplam enerji ve ekserji verimlilikleri sırasıyla %37,65 ve %39,62 olarak hesaplanmıştır. Sistem performansını artırmak için önemli göstergelerden bir tanesi de ekserji yıkım oranıdır. Sistemde meydana gelen en büyük üç ekserji yıkım oranı sırasıyla 3076 kW ile organik Rankine çevriminde, 2816 kW ile tek etkili absorpsiyonlu soğutma çevriminde ve 2658 kW ile hidrojen üretimi ve kompresyonu biriminde gerçekleşmiştir. Buna ek olarak, bazı önemli değişkenlerin sistemin performansına etkisini gözlemlemek için parametrik analiz yapılmıştır. Bu parametreler durgun hal sıcaklığı, jeotermal akışkanın kütle akış oranı, jeotermal kaynağın sıcaklığı ve ısı eşanşörü 1'in sıkışma noktası sıcaklığı olarak belirlenmiştir. Durgun hal sıcaklığında, jeotermal akışkanın kütle akış oranında ve jeotermal kaynağın sıcaklığında meydana gelen herhangi bir artışın sistem performansına olumlu etkisi olduğu, ısı eşanşörü 1'in sıkışma noktası sıcaklığındaki artışın sistemin performansını olumsuz etkilediği sonucuna ulaşılmıştır. Jeotermal kütle akış oranı 8,125 kg/s ve sıcaklığı 168 °C iken hidrojen üretim hızı 0,0024 kg/s ile maksimum seviyeye ulaşmıştır.

Anahtar kelimeler: yenilenebilir enerji, jeotermal, termodinamik, ekserji, multi-jenerasyon

How to cite this article

Yüksel, Y., E. "Thermodynamic and performance evaluation of an integrated geothermal energy based multigeneration plant", El-Cezeri Journal of Science and Engineering, 2020, 7 (2); 381-401.

Bu makaleye atıf yapmak için

Yüksel, Y., E. "Jeotermal Enerji Kaynaklı Multi-Jenerasyon Enerji Sisteminin Termodinamik ve Performans Değerlendirmesi", El-Cezeri Fen ve Mühendislik Dergisi 2020, 7 (2); 381-401.

1. Introduction

As a result of rapid increasing of population and improved life standards, energy needs of the world increase too. When current energy infrastructure is analyzed, it is seen that 80% of energy needs are met by fossil energy based systems [1]. Due to decrease in fossil source reserves and increase in environmental concerns, renewable energy systems are getting too much attention recently because of their advantages over fossil energy based systems [2,3]. Because of emissions especially CO₂, global climate changes are faced. The responsibility for those emissions is belonging to mainly fossil energy usage. 80% of CO₂ emissions are caused by coal and petroleum, on the other hand natural gas is more innocent than coal and petroleum for CO₂ emissions [4-6]. Hence, energy saving issue should be concentrated. One of the best ways of energy saving is to increase energy efficiency [7]. In this transition period of time, natural gas can be utilized for energy generation, however for long term energy politics, the use of renewables are inevitable. Geothermal energy is one of the alternatives for this long term solutions. Geothermal energy is utilized in medicine, tourism, agriculture and industry sectors [8]. Latterly, trend is to produce electricity and other useful products from geothermal energy. Kaymakcioğlu and Cirkin [9] have stated that there are 11 high temperature geothermal sources in Turkey and those sources are suitable for electricity generation. Turkey is in 7th place in the world in terms of geothermal potential. So, it is very important subject to use those geothermal potential in a correct way [10]. According to Zaim and Çavşı [11], Turkey has 861 MW installed geothermal energy plant at the end of August, 2017. Zaim and Çavşı have also compared a geothermal power plant with a conventional thermal power plant and they have suggested that for the same amount of power output if geothermal power plant is used, the CO₂ emissions would have decreased 1594.4 tons/hr. The results shared from that study have also indicated that the environmental benefits of geothermal energy.

Yılmaz and Kanoglu [12] have investigated the hydrogen production cost by using geothermal energy. The method for hydrogen production investigated in that study has been electrolysis driven by geothermal electricity. Results of the study show that as temperature and mass flow rate of geothermal sources goes up, the price of hydrogen per kilogram decreases.

Ratlamwala et. al [13] have presented an assessment analysis of new geothermal based multigeneration plant. They have stated that increasing geothermal source temperature from 167 to 227°C, hydrogen generation rate increases from 1.85 kg/day to 11.67 kg/day showing the importance of geothermal source temperature. Also, rise in geothermal source pressure increases the hydrogen production rate according to the results of paper.

Akrami et. al [14] have also proposed a multigeneration energy plant based geothermal energy source. They have performed energetic, exergetic and exergoeconomic analyses of the system with parametric analyses. They have calculated the energetic and exergetic efficiencies of plant as 34.98% and 49.17%, respectively. According to exergoeconomic analysis outputs, the lowest and highest total unit cost of outputs are 22.73 and 23.18 \$/GJ, respectively.

Al-Ali and Dincer [15] have combined solar and geothermal source together for poly-generation purposes. Energy and exergy assessments with parametric analyses are conducted for proposed multigeneration system. They have also compared the efficiencies of single generation, cogeneration, trigeneration and poly-generation systems.

In another study, Ezzat and Dincer [16] have integrated solar and geothermal energy sources for multigeneration purpose. Because of intermittency of solar energy, the plant is supported with geothermal energy source. They have evaluated the multigeneration system in terms of thermodynamic analyses. Results indicate that energy and exergy efficiency of the system are found to be 69.6% and 42.8%, respectively.

Ebadollahi et. al [17] have proposed a multigeneration system using geothermal source and LNG cold power. Thermodynamic analysis outcomes show that, the proposed multigeneration system may provide cooling, heating, power and hydrogen of 1020 kW, 334.8 kW, 1060 kW and 5.43 kg/h, respectively.

Similar study concentrated on using geothermal and solar energy has been performed by Alirahmi et. al [18]. They have performed multi-objective design optimization to evaluate the proposed system. This integrated multigeneration system has 29.95% exergy efficiency and 129.7 \$/GJ unit product cost according to the results.

In this study, it is targeted to design a novel multigeneration system producing especially hydrogen and storing it in compressed form, power, hot water, drying, heating and cooling. The novelty of this study is to increase the efficiency of the system by using waste heat of another sub-system. Also, these types of multigeneration systems are target-driven systems of which products should be necessary for the end-users living in the place in which plant is founded. Therefore it can be said that if multiple products are fitted to end-users' needs, this plant can be used by decision makers.

The main targets of this study can be listed as follows:

- To design a novel multigeneration energy system using geothermal source.
- To assess the system in terms of thermodynamic analysis especially energy and exergy efficiency.
- To determine the effects of some parameters on system performance.
- To compare the efficiencies of single generation, co-generation, tri-generation and multigeneration energy systems.

2. System Description

In order to produce multiple useful products, a novel design integrating geothermal cycle, organic Rankine cycle (ORC), hydrogen production cycle, absorption cooling cycle, hot water production and drying system together is proposed. Every stream in the multigeneration system is numerated and related equations are written. Then these equations are solved by means of Engineering Equation Solver (EES) software [19]. In this multigeneration plant, the source of the plant is geothermal energy which is shown in Fig. 1 with the number 1. Geothermal fluid firstly enters Heat exchanger (HEX) HEX 1 and mixes with water. Then the heat energy is firstly utilized in ORC 1. Produced electricity here is utilized in proton exchange membrane (PEM) electrolyzer together with the stream 15 coming from HEX 1 to heat the water before entering PEM electrolyzer. PEM electrolyzer dissolves water into hydrogen and oxygen. Produced hydrogen is stored in compressed hydrogen storage system by cooling down by means of passing through hydrogen compressors 1, 2 and 3, respectively.

The waste heat from ORC 1 is reused in ORC 2 to produce electricity. However, heat energy coming from geothermal resource passing HEX 1 is utilized in single effect absorption cooling (SEAC) cycle with stream 2. The working fluid of SEAC is selected as ammonium-water mixture (NH₃/H₂O) due to its advantage of varying the concentration. SEAC sub-plant provides cooling and heating effect by using heat energy gained from geothermal source [20]. From the generator of SEAC the stream 3 is sent to hot water storage system to transfer its heat energy to the cold water to heat it up. Then this fluid is sent to HEX 4 with the stream 4. HEX 4 helps to use waste heat to heat the air up for drying purposes. Finally, the fluid is sent back to the injection well with the stream 5. Table 1 demonstrates the input indicators for this proposed integrated geothermal based multigeneration system.

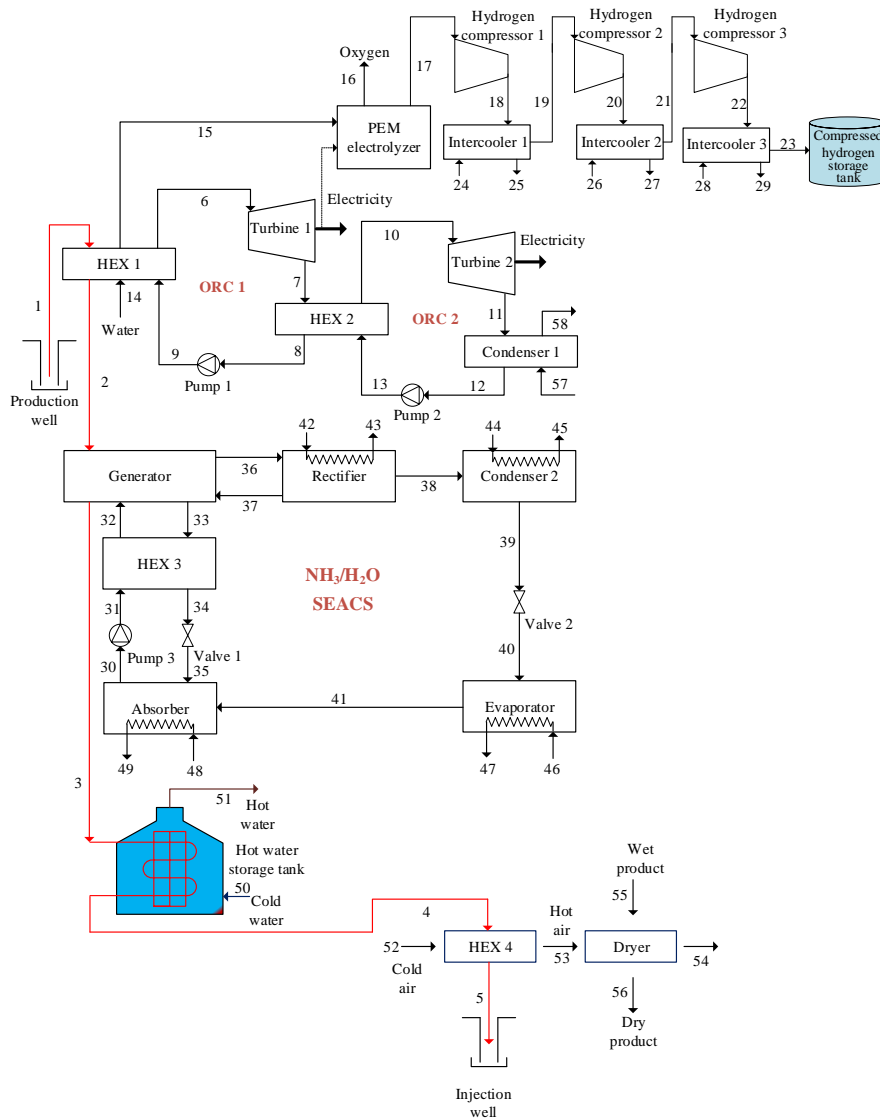


Figure 1. Schematic diagram of investigated geothermal plant for multigeneration

3. Thermodynamic Assessment

In order to analyze the control volume of any process, the mass, energy, entropy and exergy balance equalities must be considered in the design and operation of integrated plant. By defining these equations for each system and sub-systems, equalities could be solved correctly. Mass balance equality is

$$\dot{m}_{in} = \dot{m}_{out} \tag{1}$$

Here, \dot{m}_{in} and \dot{m}_{out} show the mass flow rate of input and exit. Based on the first law of thermodynamic, energetic balance equality is

$$\dot{Q}_{in} + \dot{W}_{in} + \sum \dot{m}_{in} h_{in} = \dot{Q}_{out} + \dot{W}_{out} + \sum \dot{m}_{out} h_{out} \tag{2}$$

Here, \dot{Q} and \dot{W} show heat transfer and work rate, respectively, h is specific enthalpy. Entropy balance equality is

$$\sum \dot{m}_{in} s_{in} + \sum \frac{\dot{Q}_k}{T_k} + \dot{S}_{gen} = \sum \dot{m}_{out} s_{out} \tag{3}$$

Table 1. Selected key indicators for geothermal assisted multigeneration system [21]

Input indicators	Values
Reference condition temperature, T_0	25 °C
Reference condition pressure, P_0	101.3 kPa
Geothermal working fluid production temperature, T_1	148 °C
Mass flow rate of geothermal working fluid, \dot{m}_1	8.947 kg/s
Turbine 1 inlet temperature, T_6	114 °C
Turbine 1 inlet pressure, P_6	590 kPa
Turbine 2 inlet temperature, T_{10}	52 °C
Turbine 2 inlet pressure, P_{10}	980 kPa
Isentropic efficiency of turbines, η_T	80%
Isentropic efficiency of pumps, η_p	80%
Isentropic efficiency of hydrogen compressor, η_{HC}	78%
Effectiveness of heat exchangers, ϵ_{HEX}	80%
Compressed hydrogen temperature, T_{23}	25 °C
Compressed hydrogen pressure, P_{23}	42 MPa
Temperature of PEM electrolyzer, T_{PEM}	80 °C
Working fluid of ORC 1	Isopentane
Working fluid of ORC 2	R125
Working fluid of SEAC	NH ₃ /H ₂ O
Working temperature of generator, T_{Gen}	98.55 °C
Efficiency of generator, η_{Gen}	90%
Energetic COP of SEAC, COP_{en}	0.672
Exergetic COP of SEAC, COP_{ex}	0.117
Pinch point temperature of HEX1, PP_{HEX1}	10 °C
Geothermal working fluid injection temperature, T_5	64 °C

COP: Coefficient of performance, ORC: Organic Rankine Cycle, SEAC Single effect absorption cooling

Here, s is the entropy, and \dot{S}_{gen} show entropy generation rate. Based on the second law of thermodynamic, an exergetic balance equation is

$$\sum \dot{m}_{in} ex_{in} + \dot{E}x^Q = \sum \dot{m}_{out} ex_{out} + \dot{E}x^W + \dot{E}x_D \quad (4)$$

here, $\dot{E}x^Q$ and $\dot{E}x^W$ are exergy transfer associated with heat transfer and mechanical work, respectively.

$$\dot{E}x^Q = \left(1 - \frac{T_0}{T}\right) \dot{Q} \quad (5)$$

$$\dot{E}x^W = \dot{W} \quad (6)$$

The balance equalities for integrated plant parts are defined in Table 2. To design more efficiently integrated plant, the energy and exergy efficiencies can be defined as follows; and also, performances of components of combined system are given in Table 3.

$$\eta = \frac{\text{Useful energy output in product}}{\text{Energy input}} \quad (7)$$

$$\psi = \frac{\text{Exergy output in product}}{\text{Exergy input}} \quad (8)$$

Table 2. Mass, energy, entropy and exergy balance equalities obtained from thermodynamic analysis of investigated geothermal plant

Sub-plants	Mass balance equations	Energy balance equations	Entropy balance equations	Exergy balance equations
HE X 1	$m_1 = m_2$ $m_9 = m_6$ $m_{14} = m_{15}$	$m_1 h_1 + m_9 h_9 + m_{14} h_{14}$	$m_1 s_1 + m_9 s_9 + m_{14} s_{14} +$	$m_1 ex_1 + m_9 ex_9 + m_{14} ex_{14} =$
Turbine 1	$m_6 = m_7$	$m_6 h_6 = m_7 h_7 + W_{T1}$	$m_6 s_6 + S_{g,T1} = m_7 s_7$	$m_6 ex_6 = m_7 ex_7 + W_{T1} + Ex_D$
HE X 2	$m_7 = m_8$ $m_{13} = m_{10}$	$m_7 h_7 + m_{13} h_{13} = m_8 h_8$	$m_7 s_7 + m_{13} s_{13} + S_{g,HEX2}$	$m_7 ex_7 + m_{13} ex_{13} = m_8 ex_8 +$
Pump 1	$m_8 = m_9$	$m_8 h_8 + W_{P1} = m_9 h_9$	$m_8 s_8 + S_{g,P1} = m_9 s_9$	$m_8 ex_8 + W_{P1} = m_9 ex_9 + Ex_D$
Turbine 2	$m_{10} = m_{11}$	$m_{10} h_{10} = m_{11} h_{11} + W_{T2}$	$m_{10} s_{10} + S_{g,T2} = m_{11} s_{11}$	$m_{10} ex_{10} = m_{11} ex_{11} + W_{T2} +$
Condenser 1	$m_{11} = m_{12}$ $m_{57} = m_{58}$	$m_{11} h_{11} + m_{57} h_{57} = m_{12} h_{12} + m_{58} h_{58}$	$m_{11} s_{11} + m_{57} s_{57} + S_{g,Con1}$	$m_{11} ex_{11} + m_{57} ex_{57} = m_{12} ex_{12} +$
Pump 2	$m_{12} = m_{13}$	$m_{12} h_{12} + W_{P2} = m_{13} h_{13}$	$m_{12} s_{12} + S_{g,P2} = m_{13} s_{13}$	$m_{12} ex_{12} + W_{P2} = m_{13} ex_{13} +$
PEM electrolyzer	$m_{15} = m_{16}$	$m_{15} h_{15} + W_{PEM} = m_{16} h_{16}$	$m_{15} s_{15} + S_{g,PEM} = m_{16} s_{16}$	$m_{15} ex_{15} + W_{PEM} = m_{16} ex_{16} +$
Hydrogen compressor 1	$m_{17} = m_{18}$	$m_{17} h_{17} + W_{HC1} = m_{18} h_{18}$	$m_{17} s_{17} + S_{g,HC1} = m_{18} s_{18}$	$m_{17} ex_{17} + W_{HC1} = m_{18} ex_{18} +$
Intercooler 1	$m_{18} = m_{19}$ $m_{24} = m_{25}$	$m_{18} h_{18} + m_{24} h_{24} = m_{19} h_{19} + m_{25} h_{25}$	$m_{18} s_{18} + m_{24} s_{24} + S_{g,IC1}$	$m_{18} ex_{18} + m_{24} ex_{24} = m_{19} ex_{19} +$
Hydrogen compressor 2	$m_{19} = m_{20}$	$m_{19} h_{19} + W_{HC2} = m_{20} h_{20}$	$m_{19} s_{19} + S_{g,HC2} = m_{20} s_{20}$	$m_{19} ex_{19} + W_{HC2} = m_{20} ex_{20} +$
Intercooler 2	$m_{20} = m_{21}$ $m_{26} = m_{27}$	$m_{20} h_{20} + m_{26} h_{26} = m_{21} h_{21} + m_{27} h_{27}$	$m_{20} s_{20} + m_{26} s_{26} + S_{g,IC2}$	$m_{20} ex_{20} + m_{26} ex_{26} = m_{21} ex_{21} +$
Hydrogen compressor 3	$m_{21} = m_{22}$	$m_{21} h_{21} + W_{HC3} = m_{22} h_{22}$	$m_{21} s_{21} + S_{g,HC3} = m_{22} s_{22}$	$m_{21} ex_{21} + W_{HC3} = m_{22} ex_{22} +$
Intercooler 3	$m_{22} = m_{23}$ $m_{28} = m_{29}$	$m_{22} h_{22} + m_{28} h_{28} = m_{23} h_{23} + m_{29} h_{29}$	$m_{22} s_{22} + m_{28} s_{28} + S_{g,IC3}$	$m_{22} ex_{22} + m_{28} ex_{28} = m_{23} ex_{23} +$
Generator	$m_2 = m_3$	$m_2 h_2 + m_{32} h_{32} + m_{37} h_{37}$	$m_2 s_2 + m_{32} s_{32} + m_{37} s_{37}$	$m_2 ex_2 + m_{32} ex_{32} + m_{37} ex_{37}$

or	$m_{32} + m_{37}$			
HE X 3	$m_{31} = m_{32}$ $m_{33} = m_{34}$	$m_{31}h_{31} + m_{33}h_{33} = m_{32}h_{32} + m_{33}h_{33}$	$m_{31}s_{31} + m_{33}s_{33} + \dot{S}_{g,HEX}$	$m_{31}ex_{31} + m_{33}ex_{33} = m_{32}ex_{32} + m_{33}ex_{33}$
Pump 3	$m_{30} = m_{31}$	$m_{30}h_{30} + W_{P3} = m_{31}h_{31}$	$m_{30}s_{30} + \dot{S}_{g,P3} = m_{31}s_{31}$	$m_{30}ex_{30} + W_{P3} = m_{31}ex_{31} + \dot{E}x_{D,V11}$
Valve 1	$m_{34} = m_{35}$	$m_{34}h_{34} = m_{35}h_{35}$	$m_{34}s_{34} + \dot{S}_{g,V11} = m_{35}s_{35}$	$m_{34}ex_{34} = m_{35}ex_{35} + \dot{E}x_{D,V11}$
Absorber	$m_{35} + m_{41}$ $m_{48} = m_{49}$	$m_{35}h_{35} + m_{41}h_{41} + m_{48}h_{48} = m_{49}h_{49}$	$m_{35}s_{35} + m_{41}s_{41} + m_{48}s_{48}$	$m_{35}ex_{35} + m_{41}ex_{41} + m_{48}ex_{48} = m_{49}ex_{49}$
Evaporator	$m_{40} = m_{41}$ $m_{46} = m_{47}$	$m_{40}h_{40} + m_{46}h_{46} = m_{41}h_{41} + m_{47}h_{47}$	$m_{40}s_{40} + m_{46}s_{46} + \dot{S}_{g,Eva}$	$m_{40}ex_{40} + m_{46}ex_{46} = m_{41}ex_{41} + m_{47}ex_{47}$
Valve 2	$m_{39} = m_{40}$	$m_{39}h_{39} = m_{40}h_{40}$	$m_{39}s_{39} + \dot{S}_{g,V12} = m_{40}s_{40}$	$m_{39}ex_{39} = m_{40}ex_{40} + \dot{E}x_{D,V12}$
Condenser 2	$m_{38} = m_{39}$ $m_{44} = m_{45}$	$m_{38}h_{38} + m_{44}h_{44} = m_{39}h_{39} + m_{45}h_{45}$	$m_{38}s_{38} + m_{44}s_{44} + \dot{S}_{g,Con2}$	$m_{38}ex_{38} + m_{44}ex_{44} = m_{39}ex_{39} + m_{45}ex_{45}$
Rectifier	$m_{36} = m_{37}$ $m_{42} = m_{43}$	$m_{36}h_{36} + m_{42}h_{42} = m_{37}h_{37} + m_{43}h_{43}$	$m_{36}s_{36} + m_{42}s_{42} + \dot{S}_{g,Rec}$	$m_{36}ex_{36} + m_{42}ex_{42} = m_{37}ex_{37} + m_{43}ex_{43}$
Hot water storage tank	$m_3 = m_4$ $m_{50} = m_{51}$	$m_3h_3 + m_{50}h_{50} = m_4h_4 + m_{51}h_{51}$	$m_3s_3 + m_{50}s_{50} + \dot{S}_{g,HWST}$	$m_3ex_3 + m_{50}ex_{50} = m_4ex_4 + m_{51}ex_{51}$
HE X 4	$m_4 = m_5$ $m_{52} = m_{53}$	$m_4h_4 + m_{52}h_{52} = m_5h_5 + m_{53}h_{53}$	$m_4s_4 + m_{52}s_{52} + \dot{S}_{g,HEX4}$	$m_4ex_4 + m_{52}ex_{52} = m_5ex_5 + m_{53}ex_{53}$
Dryer	$m_{53} = m_{54}$ $m_{55} = m_{56}$	$m_{53}h_{53} + m_{55}h_{55} = m_{54}h_{54} + m_{56}h_{56}$	$m_{53}s_{53} + m_{55}s_{55} + \dot{S}_{g,Dr}$	$m_{53}ex_{53} + m_{55}ex_{55} = m_{54}ex_{54} + m_{56}ex_{56}$

Table 3. Energy and exergy efficiency equalities obtained from thermodynamic analysis of investigated geothermal plant

Sub-plants	Energetic efficiency	Exergetic efficiency
HEX 1	$\eta_{HEX1} = \frac{(\dot{m}_6 h_6 - \dot{m}_9 h_9) + (\dot{m}_{15} h_{15} - \dot{m}_{14} h_{14})}{\dot{m}_1 h_1 - \dot{m}_2 h_2}$	$\psi_{HEX1} = \frac{(\dot{m}_6 ex_6 - \dot{m}_9 ex_9) + (\dot{m}_{15} ex_{15} - \dot{m}_{14} ex_{14})}{\dot{m}_1 ex_1 - \dot{m}_2 ex_2}$
Turbine 1	$\eta_{T1} = \frac{W_{T1}}{\dot{m}_6 h_6 - \dot{m}_7 h_7}$	$\psi_{T1} = \frac{W_{T1}}{\dot{m}_6 ex_6 - \dot{m}_7 ex_7}$
HEX 2	$\eta_{HEX2} = \frac{\dot{m}_{10} h_{10} - \dot{m}_{13} h_{13}}{\dot{m}_7 h_7 - \dot{m}_8 h_8}$	$\psi_{HEX2} = \frac{\dot{m}_{10} ex_{10} - \dot{m}_{13} ex_{13}}{\dot{m}_7 ex_7 - \dot{m}_8 ex_8}$
Pump 1	$\eta_{P1} = \frac{\dot{m}_9 h_9 - \dot{m}_8 h_8}{\dot{W}_{P1}}$	$\psi_{P1} = \frac{\dot{m}_9 ex_9 - \dot{m}_8 ex_8}{\dot{W}_{P1}}$
Turbine 2	$\eta_{T2} = \frac{W_{T2}}{\dot{m}_{10} h_{10} - \dot{m}_{11} h_{11}}$	$\psi_{T2} = \frac{W_{T2}}{\dot{m}_{10} ex_{10} - \dot{m}_{11} ex_{11}}$
Condenser 1	$\eta_{Con1} = \frac{\dot{m}_{11} h_{11} - \dot{m}_{12} h_{12}}{\dot{m}_{58} h_{58} - \dot{m}_{57} h_{57}}$	$\psi_{Con1} = \frac{\dot{m}_{11} ex_{11} - \dot{m}_{12} ex_{12}}{\dot{m}_{58} ex_{58} - \dot{m}_{57} ex_{57}}$
Pump 2	$\eta_{P2} = \frac{\dot{m}_{13} h_{13} - \dot{m}_{12} h_{12}}{\dot{W}_{P2}}$	$\psi_{P2} = \frac{\dot{m}_{13} ex_{13} - \dot{m}_{12} ex_{12}}{\dot{W}_{P2}}$
PEM electrolyzer	$\eta_{PEM} = \frac{\dot{m}_{H_2} LHV_{H_2}}{\dot{m}_{15} h_{15} + \dot{W}_{PEM}}$	$\psi_{PEM} = \frac{\dot{m}_{H_2} Ex_{H_2}}{\dot{m}_{15} ex_{15} + \dot{W}_{PEM}}$
Hydrogen compressor 1	$\eta_{HC1} = \frac{\dot{m}_{18} h_{18} - \dot{m}_{17} h_{17}}{\dot{W}_{HC1}}$	$\psi_{HC1} = \frac{\dot{m}_{18} ex_{18} - \dot{m}_{17} ex_{17}}{\dot{W}_{HC1}}$
Intercooler 1	$\eta_{IC1} = \frac{\dot{m}_{25} h_{25} - \dot{m}_{24} h_{24}}{\dot{m}_{18} h_{18} - \dot{m}_{19} h_{19}}$	$\psi_{IC1} = \frac{\dot{m}_{25} ex_{25} - \dot{m}_{24} ex_{24}}{\dot{m}_{18} ex_{18} - \dot{m}_{19} ex_{19}}$
Hydrogen compressor 2	$\eta_{HC2} = \frac{\dot{m}_{20} h_{20} - \dot{m}_{19} h_{19}}{\dot{W}_{HC2}}$	$\psi_{HC2} = \frac{\dot{m}_{20} ex_{20} - \dot{m}_{19} ex_{19}}{\dot{W}_{HC2}}$
Intercooler 2	$\eta_{IC2} = \frac{\dot{m}_{27} h_{27} - \dot{m}_{26} h_{26}}{\dot{m}_{20} h_{20} - \dot{m}_{21} h_{21}}$	$\psi_{IC2} = \frac{\dot{m}_{27} ex_{27} - \dot{m}_{26} ex_{26}}{\dot{m}_{20} ex_{20} - \dot{m}_{21} ex_{21}}$
Hydrogen compressor 3	$\eta_{HC3} = \frac{\dot{m}_{22} h_{22} - \dot{m}_{21} h_{21}}{\dot{W}_{HC3}}$	$\psi_{HC3} = \frac{\dot{m}_{22} ex_{22} - \dot{m}_{21} ex_{21}}{\dot{W}_{HC3}}$
Inter cooler 3	$\eta_{IC3} = \frac{\dot{m}_{29} h_{29} - \dot{m}_{28} h_{28}}{\dot{m}_{22} h_{22} - \dot{m}_{23} h_{23}}$	$\psi_{IC3} = \frac{\dot{m}_{29} ex_{29} - \dot{m}_{28} ex_{28}}{\dot{m}_{22} ex_{22} - \dot{m}_{23} ex_{23}}$
Generator	$\eta_{Gen} = \frac{\dot{m}_{33} h_{33} + \dot{m}_{36} h_{36} - \dot{m}_{32} h_{32} - \dot{m}_{37} h_{37}}{\dot{m}_2 h_2 - \dot{m}_3 h_3}$	$\psi_{Gen} = \frac{\dot{m}_{33} ex_{33} + \dot{m}_{36} ex_{36} - \dot{m}_{32} ex_{32} - \dot{m}_{37} ex_{37}}{\dot{m}_2 ex_2 - \dot{m}_3 ex_3}$
HEX 3	$\eta_{HEX3} = \frac{\dot{m}_{32} h_{32} - \dot{m}_{31} h_{31}}{\dot{m}_{23} h_{23} - \dot{m}_{24} h_{24}}$	$\psi_{HEX3} = \frac{\dot{m}_{32} ex_{32} - \dot{m}_{31} ex_{31}}{\dot{m}_{23} ex_{23} - \dot{m}_{24} ex_{24}}$
Pump 3	$\eta_{P3} = \frac{\dot{m}_{31} h_{31} - \dot{m}_{30} h_{30}}{\dot{W}_{P3}}$	$\psi_{P3} = \frac{\dot{m}_{31} ex_{31} - \dot{m}_{30} ex_{30}}{\dot{W}_{P3}}$
Valve 1	$\eta_{V1} = \frac{\dot{m}_{35} h_{35}}{\dot{m}_{24} h_{24}}$	$\psi_{V1} = \frac{\dot{m}_{35} ex_{35}}{\dot{m}_{24} ex_{24}}$
Absorber	$\eta_{Abs} = \frac{(\dot{m}_{49} h_{49} - \dot{m}_{48} h_{48})}{(\dot{m}_{30} h_{30} - \dot{m}_{35} h_{35} - \dot{m}_{41} h_{41})}$	$\psi_{Abs} = \frac{(\dot{m}_{49} ex_{49} - \dot{m}_{48} ex_{48})}{(\dot{m}_{30} ex_{30} - \dot{m}_{35} ex_{35} - \dot{m}_{41} ex_{41})}$
Evaporator	$\eta_{Eva} = \frac{\dot{m}_{47} h_{47} - \dot{m}_{46} h_{46}}{\dot{m}_{40} h_{40} - \dot{m}_{41} h_{41}}$	$\psi_{Eva} = \frac{\dot{m}_{47} ex_{47} - \dot{m}_{46} ex_{46}}{\dot{m}_{40} ex_{40} - \dot{m}_{41} ex_{41}}$
Valve 2	$\eta_{V2} = \frac{\dot{m}_{40} h_{40}}{\dot{m}_{39} h_{39}}$	$\psi_{V2} = \frac{\dot{m}_{40} ex_{40}}{\dot{m}_{39} ex_{39}}$
Condenser 2	$\eta_{Con2} = \frac{\dot{m}_{45} h_{45} - \dot{m}_{44} h_{44}}{\dot{m}_{38} h_{38} - \dot{m}_{39} h_{39}}$	$\psi_{Con2} = \frac{\dot{m}_{45} ex_{45} - \dot{m}_{44} ex_{44}}{\dot{m}_{38} ex_{38} - \dot{m}_{39} ex_{39}}$
Rectifier	$\eta_{Rec} = \frac{(\dot{m}_{26} h_{26} - \dot{m}_{27} h_{27} - \dot{m}_{38} h_{38})}{\dot{m}_{43} h_{43} - \dot{m}_{42} h_{42}}$	$\psi_{Rec} = \frac{(\dot{m}_{26} ex_{26} - \dot{m}_{27} ex_{27} - \dot{m}_{38} ex_{38})}{\dot{m}_{43} ex_{43} - \dot{m}_{42} ex_{42}}$
Hot water storage tank	$\eta_{HWST} = \frac{\dot{m}_5 h_5 - \dot{m}_4 h_4}{\dot{m}_{51} h_{51} - \dot{m}_{50} h_{50}}$	$\psi_{HWST} = \frac{\dot{m}_5 ex_5 - \dot{m}_4 ex_4}{\dot{m}_{51} ex_{51} - \dot{m}_{50} ex_{50}}$
HEX 4	$\eta_{HEX4} = \frac{\dot{m}_4 h_4 - \dot{m}_5 h_5}{\dot{m}_{53} h_{53} - \dot{m}_{52} h_{52}}$	$\psi_{HEX4} = \frac{\dot{m}_4 ex_4 - \dot{m}_5 ex_5}{\dot{m}_{53} ex_{53} - \dot{m}_{52} ex_{52}}$
Dryer	$\eta_{Dr} = \frac{\dot{m}_{56} h_{56} - \dot{m}_{55} h_{55}}{\dot{m}_{53} h_{53} - \dot{m}_{54} h_{54}}$	$\psi_{Dr} = \frac{\dot{m}_{56} ex_{56} - \dot{m}_{55} ex_{55}}{\dot{m}_{53} ex_{53} - \dot{m}_{54} ex_{54}}$

Furthermore, to make more detailed thermodynamic assessment, the energy and exergy efficiency equalities for sub-plants are written as;

Geothermal cycle;

$$\eta_{GC} = \frac{\dot{m}_1 h_1 - \dot{m}_5 h_5}{\dot{m}_1 h_1} \tag{9}$$

$$\psi_{GC} = \frac{\dot{m}_1 ex_1 - \dot{m}_5 ex_5}{\dot{m}_1 ex_1} \tag{10}$$

ORC 1;

$$\eta_{ORC1} = \frac{W_{ORC1}}{W_{P1} + (\dot{m}_6 h_6 - \dot{m}_9 h_9)} \tag{11}$$

$$\psi_{ORC1} = \frac{W_{ORC1}}{W_{P1} + (\dot{m}_6 ex_{10} - \dot{m}_9 ex_9)} \tag{12}$$

ORC 2;

$$\eta_{ORC2} = \frac{W_{ORC2}}{W_{P2} + (\dot{m}_{10} h_{10} - \dot{m}_{13} h_{13})} \tag{13}$$

$$\psi_{ORC2} = \frac{W_{ORC2}}{W_{P2} + (\dot{m}_{10} ex_{10} - \dot{m}_{13} ex_{13})} \tag{14}$$

The hydrogen production and compression;

$$\eta_{HPC} = \frac{\dot{m}_{23} h_{23}}{W_{PEM} + W_{HC1} + W_{HC2} + \dot{m}_{15} h_{15}} \tag{15}$$

$$\psi_{HPC} = \frac{\dot{m}_{23} ex_{23}}{W_{PEM} + W_{HC1} + W_{HC2} + \dot{m}_{15} ex_{15}} \tag{16}$$

The hot water production cycle;

$$\eta_{HWP} = \frac{Q_{Hot-water}}{\dot{m}_3 h_3 - \dot{m}_4 h_4} \tag{17}$$

$$\psi_{HWP} = \frac{Ex_{Hot-water}^Q}{\dot{m}_3 ex_3 - \dot{m}_4 ex_4} \tag{18}$$

The drying cycle;

$$\eta_{DC} = \frac{Q_{Drying}}{\dot{m}_{53} h_{53} - \dot{m}_{54} h_{54}} \tag{19}$$

$$\psi_{DC} = \frac{Ex_{Drying}^Q}{\dot{m}_{53} ex_{53} - \dot{m}_{54} ex_{54}} \tag{20}$$

The SEAC process;

$$\eta_{SEAC} = \frac{Q_{Cooling}}{\dot{m}_2 (h_2 - h_3) + W_{P3}} \tag{21}$$

$$\psi_{SEAC} = \frac{Ex_{cooling}^Q}{\dot{m}_2 (ex_2 - ex_3) + W_{P3}} \tag{22}$$

The equations for energy and exergy performance of single (power) production are:

$$\eta_{SG} = \frac{W_{net,SG}}{\dot{m}_1 (h_1 - h_5)} \tag{23}$$

$$\psi_{SG} = \frac{W_{net,SG}}{\dot{m}_1 (ex_1 - ex_5)} \tag{24}$$

Here, net power generation rate for single generation can be defined as follows;

$$\dot{W}_{net,SG} = (\dot{W}_{T1} + \dot{W}_{T2}) - (\dot{W}_{P1} + \dot{W}_{P2}) \quad (25)$$

The equations for energy and exergy performance of co-generation (electricity and heating) are:

$$\eta_{CG} = \frac{W_{net,SG} + Q_{Heating}}{m_1(h_1 - h_5)} \quad (26)$$

$$\psi_{CG} = \frac{W_{net,SG} + Ex_{Heating}^Q}{m_1(ex_1 - ex_5)} \quad (27)$$

Here, net power generation rate for co-generation can be defined as follows;

$$\dot{W}_{net,CG} = (\dot{W}_{T1} + \dot{W}_{T2}) - (\dot{W}_{P1} + \dot{W}_{P2}) \quad (28)$$

The equations for energy and exergy performance of tri-generation (power, heating and cooling) are:

$$\eta_{TG} = \frac{W_{net,TG} + Q_{Heating} + Q_{Cooling}}{m_1(h_1 - h_5)} \quad (29)$$

$$\psi_{TG} = \frac{W_{net,SG} + Ex_{Heating}^Q + Ex_{Cooling}^Q}{m_1(ex_1 - ex_5)} \quad (30)$$

Here, net power generation rate for co-generation can be defined as follows;

$$\dot{W}_{net,TG} = (\dot{W}_{T1} + \dot{W}_{T2}) - (\dot{W}_{P1} + \dot{W}_{P2} + \dot{W}_{P3}) \quad (31)$$

The equations for energetic and exergetic efficiency of multi-generation (power, heating, cooling, hydrogen, hot water and drying) are: (32)

$$\psi_{MG} = \frac{W_{net,SG} + Ex_{Heating}^Q + Ex_{Cooling}^Q + m_{17} ex_{H_2} + Ex_{Hot_water}^Q + Ex_{Drying}^Q}{m_1(ex_1 - ex_5)} \quad (33)$$

Here, net power generation rate for co-generation can be defined as follows;

$$\dot{W}_{net,SG} = (\dot{W}_{T1} + \dot{W}_{T2}) - (\sum \dot{W}_p + \dot{W}_{PEM}) \quad (34)$$

4. Results and Discussion

For the proposed integrated geothermal power based multigeneration system, energetic and exergetic analyses have been performed. Exergetic analysis is more useful than energetic analysis as it gives more meaningful results than energy analysis. Energy analysis also does not show the system losses. By means of exergy analysis, where and how much exergy destruction occurred can be understood. Table 3 demonstrates the energy and exergy analysis with exergy destruction rates of primary parts of proposed plant. According to the table, the lowest exergy efficiency occurs in SEAC sub-plant. The exergetic performance of whole cycle has been calculated as 39.26%.

The outputs of geothermal energy based multigeneration energy plant have been listed in Table 4. Total power productions by ORC 1 and ORC 2 have been found as 3488 kW and the cooling producing rate has been calculated as 1684 kW. With selected key indicators, hydrogen production mass flow rate is 0.0018 kg/s.

Table 3. Thermodynamic analysis results

Sub-plants/whole plant	Energetic efficiency (%)	Exergetic efficiency (%)	Exergy destruction rate (kW)	Exergy destruction ratio (%)
Geothermal cycle (GC)	40.89	42.16	1315	8.89
Organic Rankine cycle 1 (ORC 1)	32.28	20.43	3076	20.80
Organic Rankine cycle 2 (ORC 2)	25.16	14.62	1427	9.65
Hydrogen production and compression (HPC)	47.34	44.57	2658	17.98
t water production (HWP)	69.24	66.38	2169	14.67
Drying cycle (DC)	74.18	71.26	1324	8.96
Single effect absorption cooling (SEAC)	14.92	12.14	2816	19.05
Whole system (WS)	37.65	39.26	14785	100

Table 4. Geothermal energy-based power plant outputs

Plant outputs	Values
Power production rate of ORC 1, W_{ORC1}	2683 kW
Power production rate of ORC 2, W_{ORC2}	805 kW
Cooling producing rate, $Q_{Cooling}$	1684 kW
Heating producing rate, $Q_{Heating}$	846 kW
Hot water production capacity, Q_{Hot_water}	3042 kW
Drying production capacity, Q_{Drying}	1126 kW
Produced hydrogen mass flow rate, $m_{Hydrogen}$	0.0018 kg/s

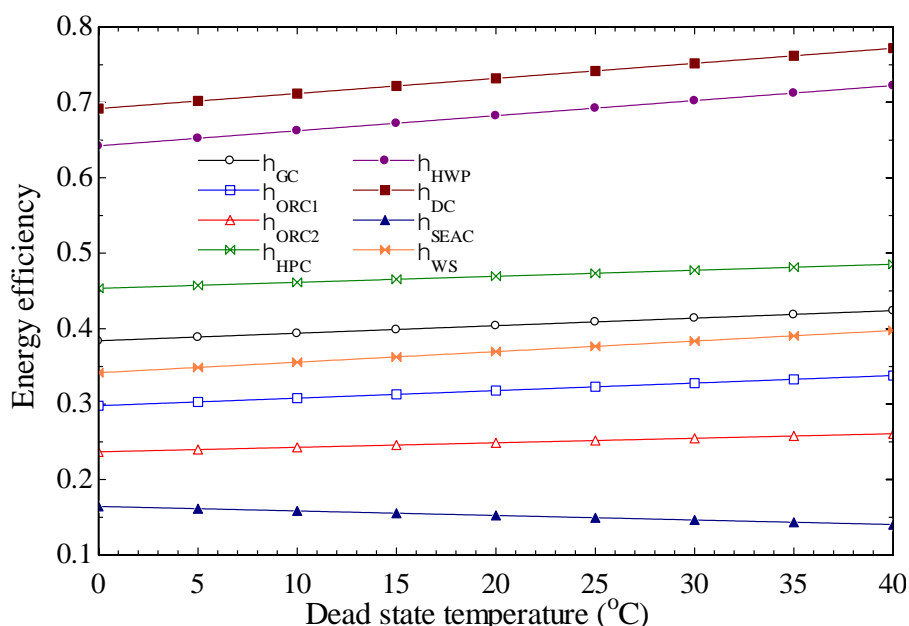


Figure 2. Variation in energy performances of whole plant and its sub-plants versus dead state temperature

4.1 Effect of Dead State Temperature

In order to investigate the impacts of some indicators on system performance, parametric analysis has been done. The first parameter calculated is dead state temperature. Fig. 2 illustrates the impact of dead state temperature on energetic efficiencies of sub-plants and whole system. According to the analysis results, energetic efficiencies of all sub-plants and whole system except for SEAC increase with increasing dead state temperature. The reason behind this situation is that when dead state temperature increases, cooling load of SEAC cycle increases too.

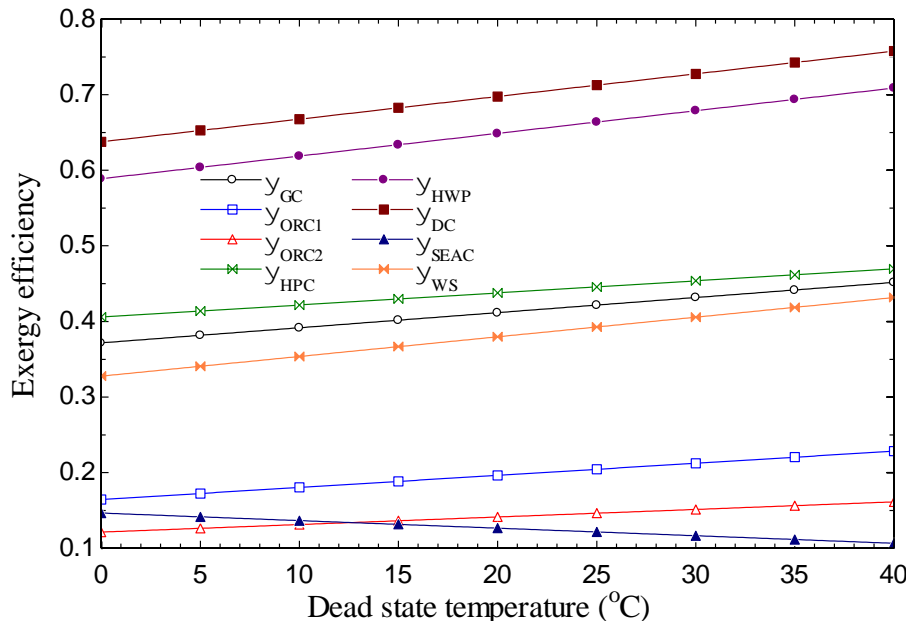


Figure 3. Variation in exergy efficiencies of whole plant and its sub-plants versus dead state temperature

Fig. 3 demonstrates how exergetic efficiencies of sub-plants and whole plant vary with respect to increasing dead state temperature. Similar to energy analysis results, while dead state temperature increases, exergy performances of whole system and sub-plants except for SEACs increase too. As a result of these analyses, it can be said that increasing dead state temperature has positive impact on performance of the proposed plant.

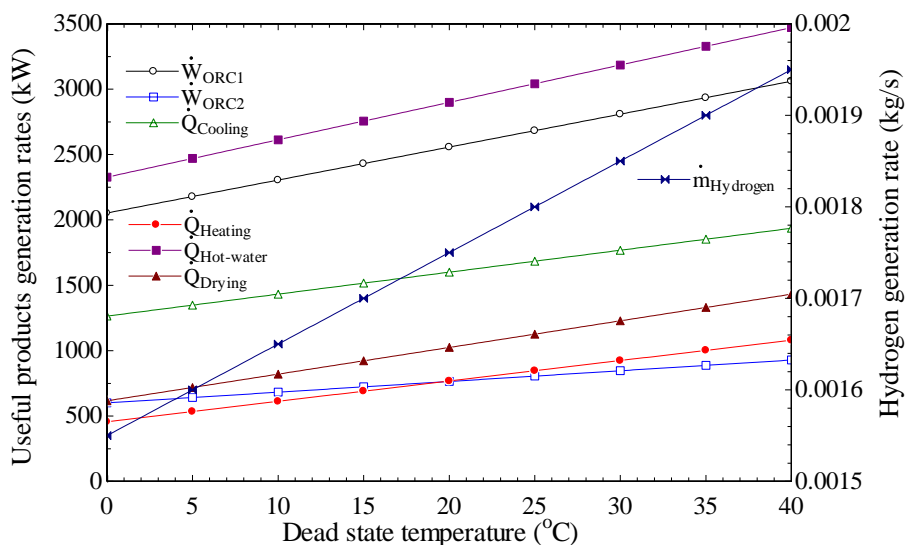


Figure 4. Variation in useful outputs from geothermal plant versus dead state temperature

As mentioned before, increasing dead state temperature has positive impact on plant performance and this positive effect can be seen on product generation rates. As dead state temperature rises from 0 to 40°C, hydrogen production rate rises from about 0.00155 to 0.00196 kg/s. As seen from the figure, with increasing dead state temperature products of ORCs, cooling and heating, hot water and drying increase as well. Having investigated power production by ORC 1 and ORC 2, it is seen that power production of ORC 1 increases from nearly 2000 to 3000 kW and power production of ORC 2 rises from 650 to approximately 850 kW. The reason of those increases in both efficiencies and production rates can be explained by the definition of thermodynamic efficiencies. As the difference between ambient temperature and working temperature of any unit decreases, losses will be decreased.

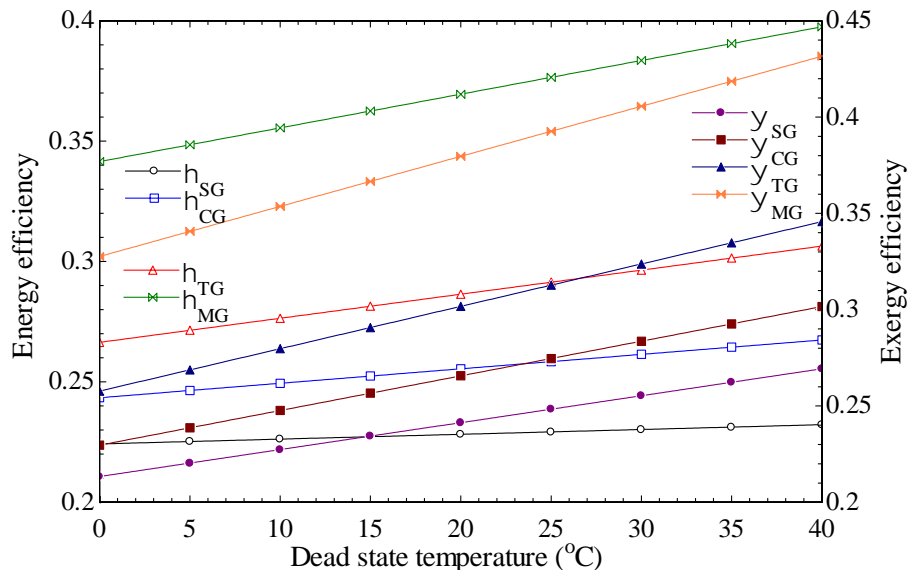


Figure 5. Variation in energetic and exergetic efficiencies of SG, CG, TG and MG options versus dead state temperature

Figure 5 demonstrates the importance of using multigeneration for energy plants. Producing more than three outputs by using waste heat again and again increases the performance of energy production systems. As seen from the figure, while dead state temperature rises from 0 to 40 °C, energetic and exergetic efficiencies of single generation plant rise slightly. However, energy performance of multigeneration plant increases from 34% to 40% and exergetic efficiency of multigeneration plant rises 34% to nearly 44%.

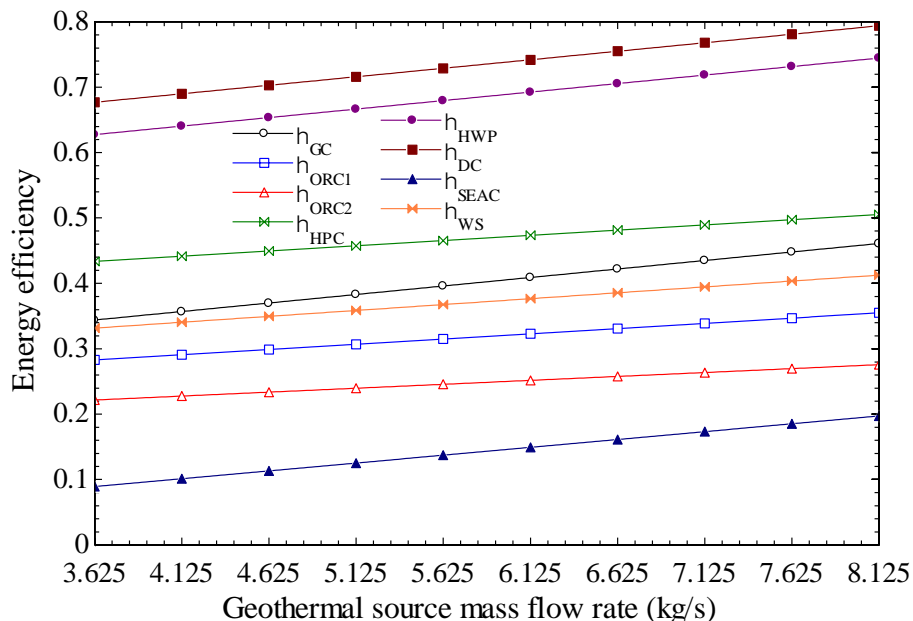


Figure 6. Energetic efficiencies of geothermal plant and its sub-plants vs geothermal source mass flow rate

4.2 Effect of Geothermal Source Mass Flow Rate

As another significant indicator affecting system efficiency, geothermal source mass flow rate is investigated in this part. As seen from Figure 6, while geothermal source mass flow rate rises from 3.625 to 8.125 kg/s, all sub-plants and whole plant are affected positively in terms of energy efficiency.

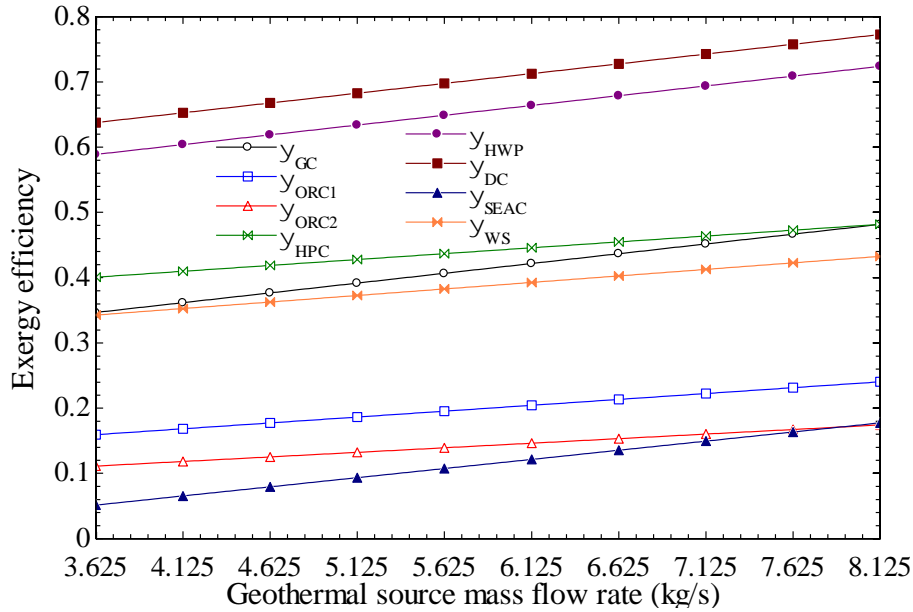


Figure 7. Exergetic efficiencies of geothermal system and its sub-systems vs geothermal source mass flow rate

Figure 7 shows the exergy efficiencies change with respect to increasing geothermal source mass flow rate. Results of figure state that increasing mass flow rate of geothermal source has also positive effect on exergy efficiencies of sub-plants and whole plant. As geothermal source mass flow rate goes up to 8.125 kg/s, exergy efficiency of whole system increases nearly from 34% to almost 42% due to increase in mass input per time to the sub-systems of the multigeneration system.

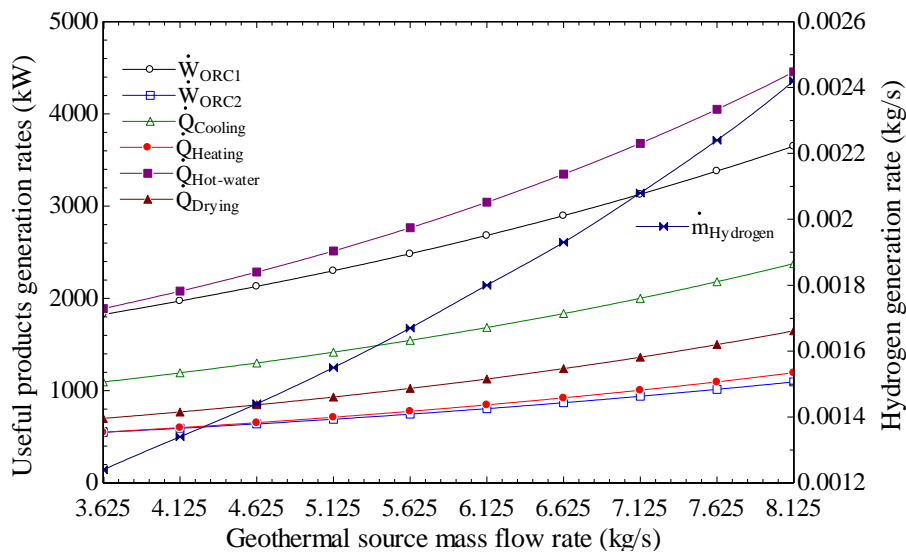


Figure 8. Useful outputs from geothermal plant vs geothermal source mass flow rate

One of the most significant products of this proposed plant is hydrogen which is affected positively with increasing geothermal source mass flow rate from 3.625 to 8.125 kg/s. hence, hydrogen production rate doubles from 0.0012 to 0.0024 kg/s for this range. Similar to hydrogen generation, other products such as power, heating and cooling, hot water and drying raise with increasing geothermal source mass flow rate because this increase in mass flow rate carries more enthalpy.

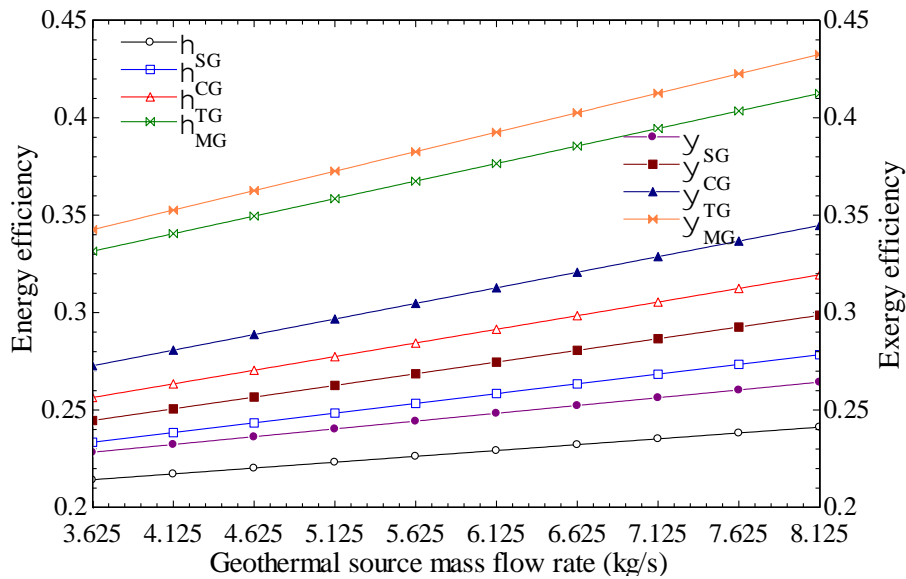


Figure 9. Energetic and exergetic efficiencies of SG, CG, TG and MG options vs geothermal source mass flow rate

Figure 9 illustrates the similar results as Figure 5. As mass flow rate increases energetic and exergetic efficiencies of all energy generation plant types increase as well. It can be surely said that efficiencies of multigeneration energy plants are higher than any other types. The other result to be drawn from that figure is that increase in geothermal source mass flow rate has positive impact on all types of production systems for given range.

4.3 Effect of Geothermal Source Temperature

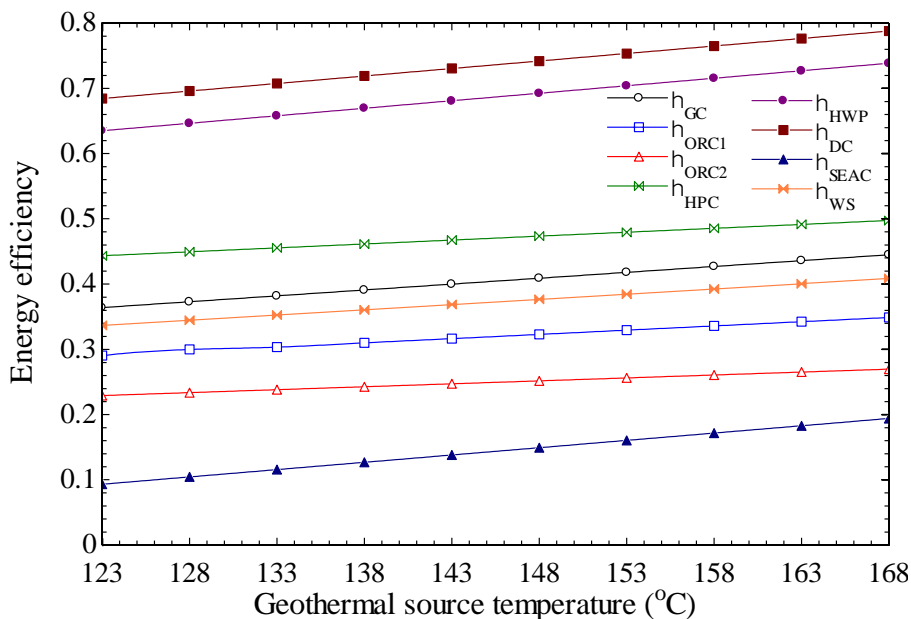


Figure 10. Effects on the energy efficiencies of the geothermal source temperature for the geothermal system and its sub-systems

Figure 10 shows the impact of geothermal resource temperature on energy efficiencies of sub-plants and whole plant. As seen from the figure, while geothermal resource temperature rises from 123 to 168 °C, energetic performances of sub-plants and whole system increase too.

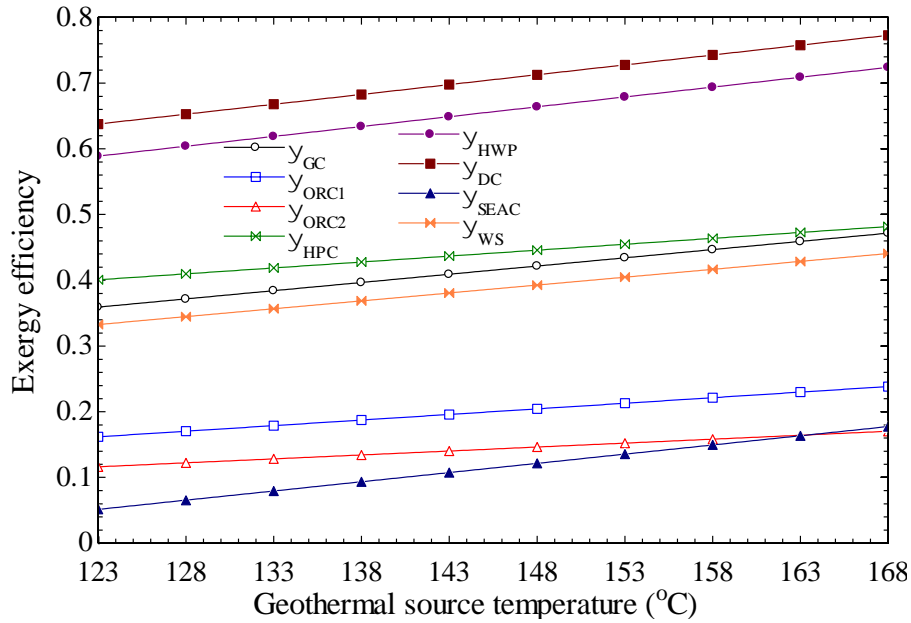


Figure 11. Effects on the exergy efficiencies of the geothermal source temperature for the geothermal plant and its sub-plants

Like energetic performance, exergetic efficiencies of sub-plants and whole system increase with increasing geothermal source temperature. Because higher temperature in geothermal source means higher enthalpy it carries. As seen from the figure, especially hot water production and drying cycle boost with increasing geothermal fluid temperature. Exergy efficiency of drying cycle reaches up to 78% when geothermal source temperature is 168 °C.

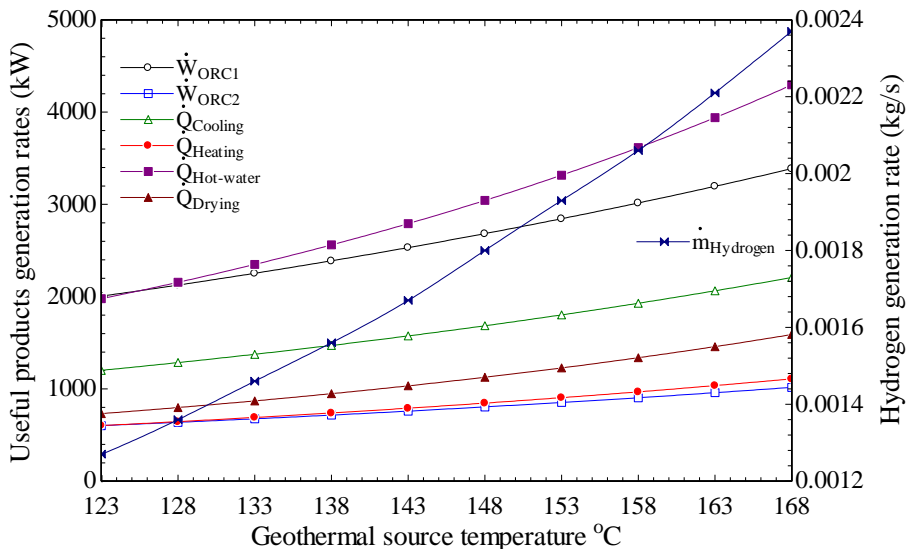


Figure 12. Effects on the useful products and hydrogen generation rate of the geothermal source temperature for the geothermal plant

Useful product generation rates also rise with rising geothermal resource temperature as seen from Figure 12. Hydrogen production rate increases from 0.0013 to 0.0024 kg/s. Any increase in geothermal source temperature makes enthalpy higher. Then useful productions and efficiencies can go up due to that enthalpy increase.

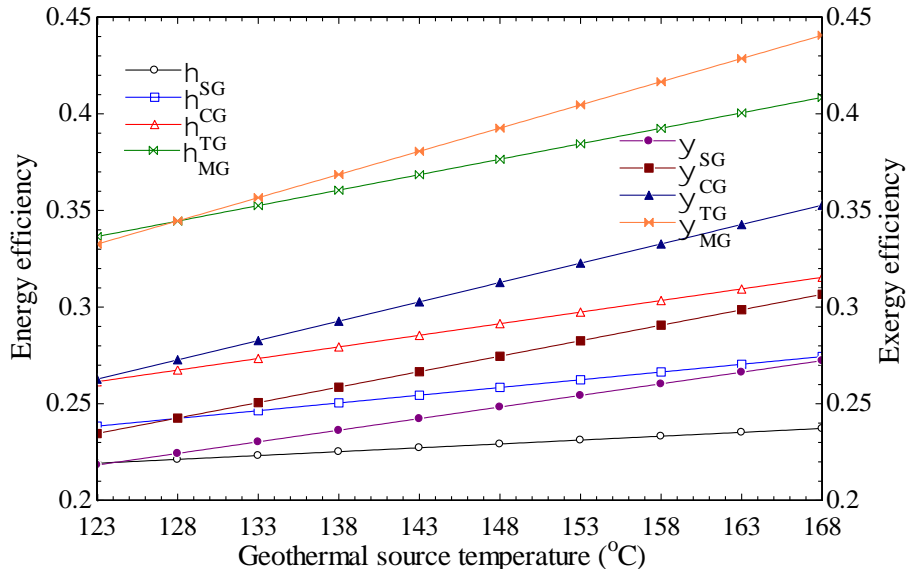


Figure 13. Effects on the energetic and exergetic efficiencies of the geothermal source temperature for the SG, CG, TG and MG options

Figure 13 illustrates the impact of increasing geothermal resource temperature on different types of generation systems’ energetic and exergetic efficiencies. In each case, energy and exergy efficiencies of generation systems are affected positively with increasing geothermal source temperature.

4.4 Effect of Pinch Point Temperature of HEX 1

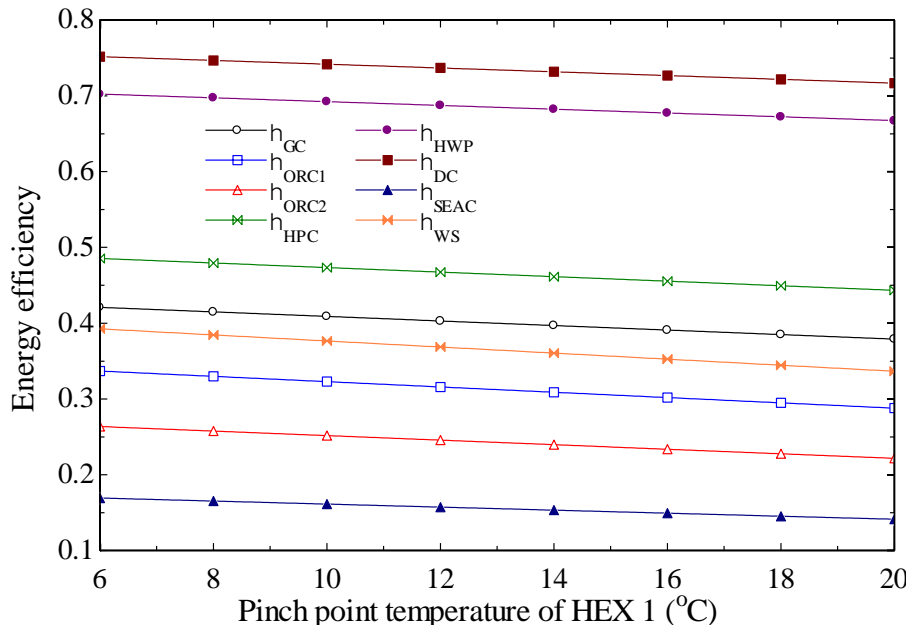


Figure 14. The impact of pinch point temperature of HEX 1 on the energetic efficiencies of geothermal system and its sub-systems

Figure 14 and 15 reveals how energetic and exergetic efficiencies of sub-systems and whole system vary with changing pinch point temperature of HEX 1, respectively. As pinch point temperature of HEX 1 increases from 6 to 20 °C, energy and exergy performances of sub-plants and whole system decrease.

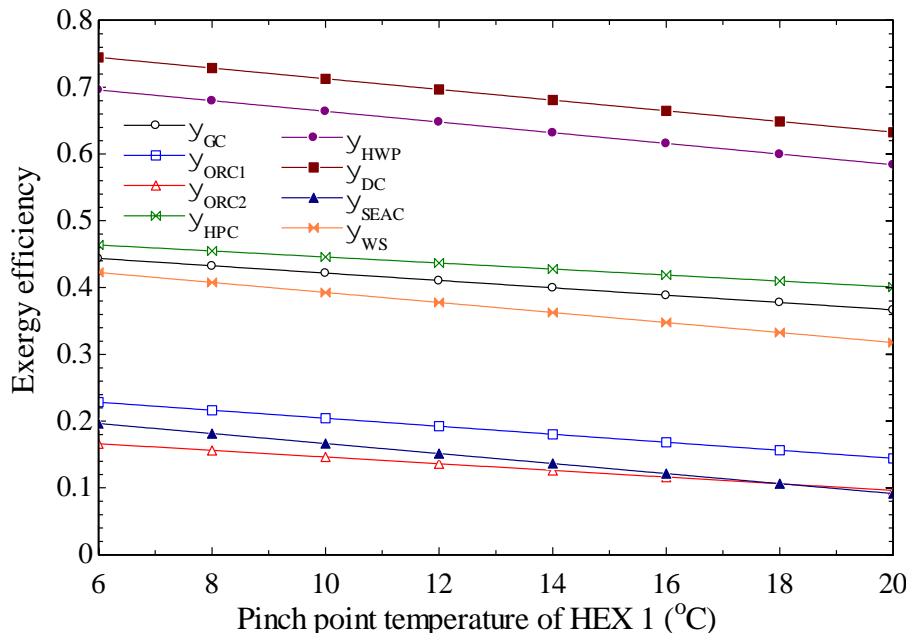


Figure 15. The impact of pinch point temperature of HEX 1 on the exergy efficiencies of geothermal system and its sub-systems

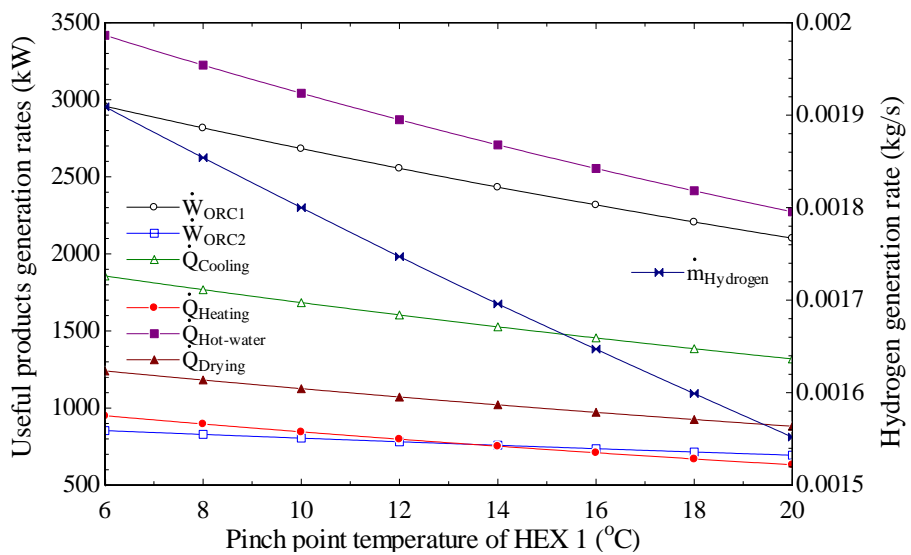


Figure 16. The impact of pinch point temperature of HEX 1 on the useful products and hydrogen generation rates from geothermal plant

Because energy and exergy efficiencies decrease with rising pinch point temperature of HEX 1, useful product generation also decrease for this increase in pinch point temperature on HEX 1 as illustrated in Figure 16.

Finally, Figure 17 illustrates the negative effects of increasing pinch point temperature of HEX 1 on energy and exergy performances of different ways of production plants. For instance, energy efficiency of multigeneration plant decreases from nearly 40% to about 33%, and exergy efficiency of MG plant goes down nearly to 32% from 43%.

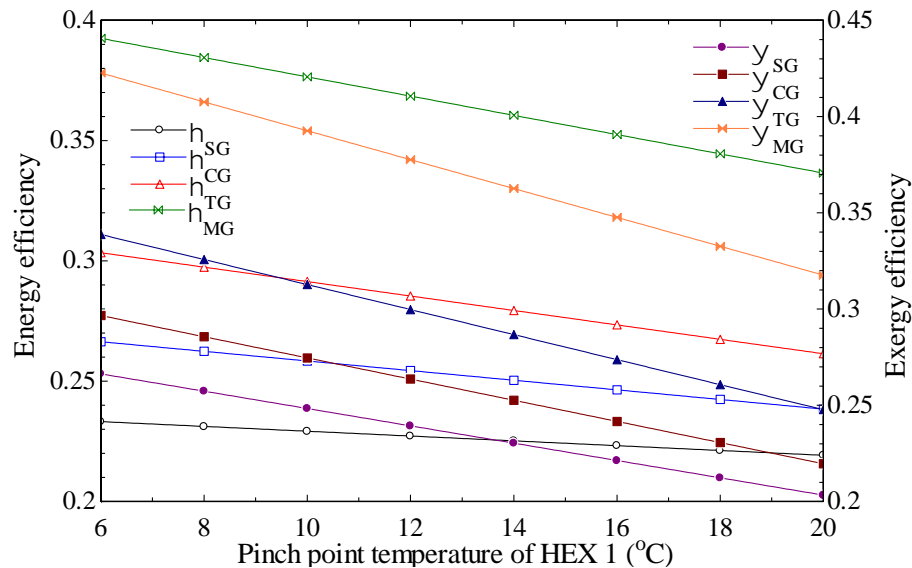


Figure 17. The impact of pinch point temperature of HEX 1 on the energetic and exergetic performances of SG, CG, TG and MG options

5. Conclusions

In this study, it is targeted to set a new integrated plant based on geothermal power for multigeneration purposes. Multiple products such as hydrogen, power, hot water, drying, cooling and heating are generated by using geothermal energy and waste heat of the system. For thermodynamic evaluation of the system, each stream in the proposed system is numbered and thermodynamic balance equations are assigned to them. Then for every single unit of the system, balance equations which are mass, energy, entropy and exergy are calculated to find the energy and exergy performances of sub-systems out. Based on the analysis results, energy and exergy analyses of whole plant are computed as 37.65% and 39.26%. Other striking numerical results are as follows:

- Two most important parameters affecting system performance and mainly hydrogen generations are mass flow rate and temperature of geothermal resource. As geothermal source temperatures reach up to 168°C, hydrogen generation rates maximize to 0.0024 kg/s, exergetic performance of system increases up to 44%.
- As geothermal mass flow rate goes up to 8.125 kg/s, hydrogen production rates again reaches to 0.0024 kg/s and exergetic performance of the whole plant rises to 43.7%.
- Dead state temperature has also positive impacts on energetic and exergetic analyses of all sub-plants and whole plants owing to decrease of losses caused by temperature differences between environment and the system.
- As pinch point temperature of HEX 1 goes up to 20°C, energy efficiency, exergy efficiency and useful product generation rates decrease.

In the light of those outcomes of thermodynamic and parametric analyses, it can be concluded that this type of a geothermal based multigeneration system can be effective to provide human needs especially for district areas. Naturally, geothermal based multigeneration system will be effective for places where geothermal sources are found, however those products provided by the multigeneration system proposed in this study are necessary for society. While energy plants were single generation, they had less efficiency. Then trends gravitate towards cogeneration and tri-generation energy plants. In near future, use of these types of multigeneration energy plants will be inevitable.

References

- [1]. Office of Energy Analysis. "US-EIA International Energy Outlook". Washington DC, USA, 2013. O
- [2]. zturk, M.; Yuksel, Y. E., Energy structure of Turkey for sustainable development, Renewable and Sustainable Energy Reviews, 2016, 53: 1259-1272. O
- [3]. örgülü S. Burdur İlinin Hayvansal ve Bazı Tarımsal Atık Kaynaklı Biyogaz Potansiyelinin Belirlenmesi. El-Cezeri Journal of Science and Engineering. 2019; 6(3): 557-543. G
- [4]. International Energy Agency. "Technical Report 2012 Key World Energy Statistics". 2012. <http://www.iea.org/publications/freepublications/publication/KeyWorld2014.pdf>. (05.09.2015). I
- [5]. OMRI R . Energy and Exergy Analyses of Different Transcritical CO2 Refrigeration Cycles. El-Cezeri Journal of Science and Engineering. 2018; 5(2): 436-425. G
- [6]. kyürek Z . Energy Recovery and Greenhouse Gas Emission Reduction Potential of Bio-Waste in the Mediterranean Region of Turkey. El-Cezeri Journal of Science and Engineering. 2019; 6(3): 490-482. A
- [7]. ahçeci, S.; Daldaban, F., Economic Analysis of Demand Side Management with Residential PV System and Energy Storage System. El-Cezeri Journal of Science and Engineering, 2020, 7(1): 67-78. B
- [8]. ulekci, O.C., Yenilenebilir enerji kaynakları arasında jeotermal enerjinin yeri ve Türkiye açısından önemi, Ankara Üniversitesi Çevre Bilimleri Dergisi, 2009, 1(2): 83-91. K
- [9]. aymakcioglu, F.; Cirkin T., Jeotermal Enerjinin Değerlendirilmesi ve Elektrik Üretimi, III. Yenilenebilir Enerji Kaynakları Sempozyumu ve Dergisi Bildiriler Kitabı, 2005, 19-21. K
- [10]. ilmaz, M., Türkiye'nin enerji potansiyeli ve yenilenebilir enerji kaynaklarının elektrik enerjisi üretimi açısından önemi, Ankara Üniversitesi Çevrebilimleri Dergisi, 2012, 4(2): 33-54. Y
- [11]. aim, A.; Çavşi, H., Türkiye'deki Jeotermal Enerji Santrallerinin Durumu, Mühendis ve Makina. 2018, 59 (691): 58-45. Z
- [12]. ilmaz, C.; Kanoglu, M., Investigation of hydrogen production cost by geothermal energy, International Advanced Researches and Engineering Journal, 2017, 1(1): 10-5. Y
- [13]. atlamwala, T.A.H.; Dincer, I.; Gadalla, M.A., Performance analysis of a novel integrated geothermal-based system for multi-generation applications, Applied Thermal Engineering, 2012, 40: 71-79. R
- [14]. krami, E.; Chitsaz, A.; Nami, H.; Mahmoudi, S.M.S., Energetic and exergoeconomic A

- assessment of a multi-generation energy system based on indirect use of geothermal energy, *Energy*, 2017, 124: 625-639.
- [15]. l-Ali, M.; Dincer, I., Energetic and exergetic studies of a multigenerational solar–geothermal system, *Applied Thermal Engineering*, 2014, 71(1): 16-23. A
- [16]. zzat, M.F.; Dincer, I., Energy and exergy analyses of a new geothermal–solar energy based system, *Solar Energy*, 2016, 134: 95-106. E
- [17]. badollahi, M.; Rostamzadeh, H.; Pedram, M.Z.; Ghaebi, H.; Amidpour, M., Proposal and assessment of a new geothermal-based multigeneration system for cooling, heating, power, and hydrogen production, using LNG cold energy recovery, *Renewable Energy*, 2016, 135: 66-87. E
- [18]. lirahmi, S. M.; Dabbagh, S.R.; Ahmadi, P.; Wongwises, S., Multi-objective design optimization of a multi-generation energy system based on geothermal and solar energy, *Energy Conversion and Management*, 2020, 205: 112426 A
- [19]. lein S.A.; Alvarado F.L., *Engineering Equation Solver, F-Chart Software*, Madison, WI. 2002, 1. K
- [20]. zen, D.N.; Yağcıoğlu, K., Thermodynamic and Exergy Analysis of an Absorption Cooling System for Different Refrigerants, *El-Cezerî Journal of Science and Engineering*, 2020, 7(1): 93-103. Ö
- [21]. badollahi, M.; Rostamzadeh, H.; Pedram, M.Z.; Ghaebi, H.; Amidpour, M., Proposal and assessment of a new geothermal-based multigeneration system for cooling, heating, power, and hydrogen production, using LNG cold energy recovery, *Renewable energy*, 2019, 135: 66-87. E